A New Wavelet Based Image Denoising Method

Jin Quan*, William G. Wee* and Chia Y. Han+

*School of Electronic and Computing Systems, University of Cincinnati, Cincinnati, OH 45221, USA

+School of Computing Sciences and Informatics, University of Cincinnati, Cincinnati, OH 45221, USA

Abstract

This paper proposes a new wavelet based image denoising method by using linear elementary parameterized denoising functions in the form of derivatives of Gaussian of a set of estimated wavelet coefficients. These coefficients are derived from an improved context modeling procedure in terms of mean square error estimation combining inter- and intra-subband data. The denoising method results in a two-step denoising effort which outperforms the state-of-the-art non-redundant methods. This method is also extended to the overcomplete wavelet expansion by applying cycle spinning, which provides additional denoising performance and yields significantly better results than the orthogonal transform.

1. Introduction

Achieving preferable performances for image compression usually requires an efficient representation of images. To assure an efficient representation of images in scientific and commercial applications, image denoising is a favorable processing step. A general solution approach is to convert the contaminated image into another domain through a transformation and perform the denoising operations in that domain before converting back to the original image domain.

Currently, one of the best approaches used for denoising is to use the wavelet transforms. Given a noisy signal *y*, as the sum of the original signal *x* and the noise *b*, a discrete wavelet transform (*DWT*) is applied on this contaminated signal data to produce subbands of wavelet coefficients. The most commonly used denoising method based on wavelet coefficients is the soft thresholding strategy, which has been theoretically justified by Donoho and Johnstone in [1,2]. Most importantly, they have derived a minimax square error bound for soft thresholding functions that depend on data sample size and the level of additive Gaussian noise contamination. Some seminal works include [3-5].

2. Motivations

The theoretical result of Donoho and Johnstone in [1,2] shows that

$$E \| \hat{y} - x \|_{2,N}^2 \le \Lambda_N \{\varepsilon^2 + \sum_{i=1}^{N} \min(y_i^2, \varepsilon^2)\} \quad (1)$$

for all $x \in R^n$, and for an estimation: $\hat{y}_i = \eta_s(y_i, \lambda_N \varepsilon)$ (2)

where

$$\eta_s(y_i, \lambda_N \varepsilon) = \mathrm{sgn}(\lambda_N \varepsilon)(|y_i| - \lambda_N \varepsilon)_+$$

$$\| \hat{y} - x \|_{2,N}^2 = \sum_{i=1}^{N} (\hat{y} - x)_i^2$$

$y_i = x_i + b_i = x_i + \varepsilon d_i, i = 1,2,..N$ the noise level $\varepsilon > 0$ and d_i are i.i.d. $N(0,1)$. And $\lambda_N \le (2 \log N)^{1/2}$ and $\Lambda_N \le 2 \log \log N + 1$ for N total samples.

Eq(1) means that in order to achieve the minimax upper bound of $E \| \hat{y} - x \|_{2,N}^2$ the soft thresholding function Eq(2) has to be followed.

As indicated in the typical denoising flow chart shown in Figure 1 [5], to apply discrete wavelet transform (*DWT*) to the noisy image data $Y = (Y_i), i \in [1, N]$ is to produce *J* noisy wavelet subband (subimage) $Y^j = (Y_i^j), i \in [1, N_j], j \in [1, J]$. The denoising operation is to produce $\hat{x}^1 \ldots \hat{x}^j \ldots \hat{x}^J$ with each being an estimator of x^j, and the inverse discrete wavelet transform(*IDWT*) is to produce estimate of the noise free data *x*. The additive noise *b* is Gaussian noise with the distribution of $N(0, \sigma^2)$.

To summarize, our research motivation is to reduce the square error upper bound of Eq(1) so that the resulting procedure has the largest denoising effect in terms of PSNR.

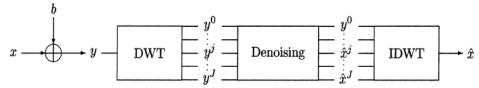

Figure 1: A wavelet denoising flowchart

3. Proposed solution

Based on the motivations, we split the minimization of the squared error between the estimate and the original data into two separated operations: 1).To reduce $\sigma_n(y)$. 2).To optimize the soft thresholding denoising function.

For Operation 1, our suggestion is to apply a linear estimator like: $Z_i^j = (\bar{w}^j)^t \bar{u}_i^j$ (3)

where is the subband parameter vector derived from :

$$\bar{w}^j = \arg\min_{\bar{w}} \sum_{N_j} (|Y_i^j| - (\bar{w}^j)^t \bar{u}_i^j)^2 \quad (4)$$

and $\bar{u}_i^j$ is a vector composed by certain wavelet coefficients.

Thus Z does not degrade the signal X but results in a lower noisy standard deviation. A good candidate for Z could be the smoothing estimator using context modeling proposed in [4]. However, we improve it by the following.

We perform a 4-level DWT operation on the incoming noise image y, to produce Y with subband designations shown in Figure 2. For Subband 1-6, use a neighborhood to build up a 34 by 1 vector. For Subband 7-12, just use a neighborhood of size 3 by 3 to build up a 9 by 1 vector. Meanwhile, instead of directly applying *Z* as an alternate of *Y* in the optimization of soft thresholding operation, we add portion of *Y* to this *Z* so that to construct a newer smoothed version. The expression would be like below where values of A are listed in Table 1.

$$Z_{new} = A \times Z + (1 - A) \times Y \quad (5)$$

For Operation 2, a soft thresholding denoising operator with a linear combination of parameterized derivative of Gaussian (*DOG*) formulations was proposed in [5]. Although the analytical solution given in [5] is neither directly applicable on *Z* nor *Znew*, we can still use it to derive an alternate by applying additional offset values on these solutions in order to obtain the final weights in the following expression:

$$\hat{X} = (a_1 + a_2 \times e^{\frac{-Z_{new}^2}{12\sigma^2}}) \times Z_{new} \quad (6)$$

where $a_1 = a_1' + \Delta a_1, a_2 = a_2' + \Delta a_2$ and $a' = M^{-1} c$ where $a' = (a_1', a_2')^T$

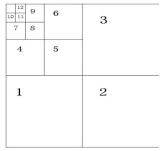

Figure 2: Subband designations

Table 1: Values of *A* at different subbands and noise levels.

	Subbands			
Noise Level	1-3	4-6	7-9	10-12
[0,5)	0.5	0.2	0.05	0
[5,10)	0.7	0.4	0.15	0.05
[10,15)	0.7	0.45	0.2	0.05
[15,20)	0.7	0.5	0.3	0.1
[20,25)	0.75	0.55	0.35	0.15
[25,30)	0.8	0.6	0.4	0.2
[30,50)	0.9	0.8	0.6	0.3
[50,100]	0.9	0.8	0.7	0.5

Table 2: Values of delta a1 under different subbands and noise levels.

	Subbands			
Noise level	1-3	4-6	7-9	10-12
[0,5)	0.2	0.1	0	0
[5,10)	0.3	0.2	0.1	0
[10,15)	0.2	0.3	0.1	0
[15,20)	0.2	0.3	0.2	0.1
[20,25)	0.1	0.4	0.2	0.1
[25,30)	0.1	0.4	0.3	0.1
[30,50)	0.1	0.3	0.4	0.1
[50,100]	0	0.2	0.4	0.3

Table 3: Values of delta a2 under different subbands and noise levels.

	Subbands			
Noise level	1-3	4-6	7-9	10-12
[0,5)	0.1	0	0	0.1
[5,10)	0.1	0	0	0.1
[10,15)	0.1	0	0	0.1
[15,20)	0.1	0	0	0.1
[20,25)	0.1	0	0	0.1
[25,30)	0.1	0	0	0.1
[30,50)	0	0	0	0.1
[50,100]	0.1	0	0	0.1

$$M = \begin{pmatrix} Y^2 & Y^2 \times e^{\frac{Y^2}{12\sigma^2}} \\ Y^2 \times e^{\frac{Y^2}{12\sigma^2}} & Y^2 \times e^{\frac{Y^2}{6\sigma^2}} \end{pmatrix} \quad c = \begin{pmatrix} Y^2 - \hat{\sigma}^2, [Y^2 - \hat{\sigma}^2 (1 - \frac{Y^2}{6\sigma^2})] \times e^{\frac{Y^2}{12\sigma^2}} \end{pmatrix}^T$$

The values of delta a1 and delta a2 can be obtained from experimental results, which we list based on different noise levels and subband groups in Table 2 and Table 3, respectively.

4. Overcomplete expansion

One may often observe Pseudo-Gibbs phenomena in the area of edge and ridge discontinuities in images after standard wavelet denoising. These disturbing visual artifacts are generally caused by the shift variance, an intrinsic drawback of DWT. According [6], the actual positions of the image discontinuities play a significant role for the sizes of these artifacts.

Since the artifacts are highly related to the alignment between the features in the signal and the features of basis wavelet applied, it is easy to reason that similar signals but with only a different alignment would generate fewer artifacts after being wavelet denoised. Thus, by carrying out the procedure called *cycle spinning* [6], we can shift the signal to change the positions of features, so that the artifacts produced in the denoised image can be diminished by re-aligning the given noisy image. In cases of 2D signal, translation-invariance can be achieved by shifting the pixels of columns and/or rows. Usually only a small number of shifts like 20~30 may be sufficient in practice.

5. Results

Our proposed method is compared with the *SURE-LET* [5], which is the most efficient denoising technique available based on non-redundant orthogonal wavelet transform. Table 4 summarizes the results, which show that our method carries about 0.4~1 dB improvement on average. And the computation time is around 3~5 seconds on a regular PC for the whole denoising process.

In addition, in order to demonstrate the denoising efficiency of the proposed method when applying overcomplete expansion, we show the denoising results of the six images in Table 5 using *BLS-GSM* [3], *SURE-LET* [8] and *BM3D* [7], which is a non-wavelet state-of-the-art denoising approach. We also provide a set of images for visual comparison.

Table 4 : Comparison on PSNR (dB) with *SURE-LET* (non-redundant).

Noise level	5	10	15	20	25	30	50	100
Input PSNR	34.15	28.13	24.61	22.11	20.17	18.59	14.15	8.13
Method	**Lena**							
SURE-LET	37.96	34.56	32.68	31.37	30.36	29.56	27.37	24.66
Proposed Method	38.92	35.42	33.50	31.89	31.16	30.32	28.17	25.32
Method	**Boat**							
SURE-LET	36.70	32.90	30.85	29.47	28.44	27.63	25.50	22.97
Proposed Method	37.14	33.65	31.70	30.28	29.23	28.50	26.40	24.10
Method	**Goldhill**							
SURE-LET	36.53	32.69	30.76	29.52	28.60	27.89	26.06	23.82
Proposed Method	37.62	34.02	32.17	30.87	30.10	29.50	27.80	25.47
Method	**Man**							
SURE-LET	36.95	32.87	30.78	29.44	28.47	27.71	25.76	23.42
Proposed	37.56	33.56	31.59	30.28	29.49	28.72	27.03	24.71

Table 5: Comparison on PSNR (dB) with some most efficient denoising methods.

Noise level	5	10	15	20	25	30	50	100
Input PSNR	34.15	28.13	24.61	22.11	20.17	18.59	14.15	8.13
Method	**Lena**							
SURE-LET*	38.25	35.08	33.31	32.06	31.10	30.33	28.22	25.57
BLS-GSM*	38.49	35.61	33.90	32.66	31.69	30.46	28.61	25.64
BM3D	38.72	35.93	**34.27**	33.05	**32.08**	**31.26**	28.86	25.57
Proposed	**39.36**	**36.10**	34.08	**32.65**	31.81	30.98	**28.87**	**25.95**
Method	**Boat**							
SURE-LET	37.13	33.53	31.57	30.22	29.20	28.39	26.20	23.61
BLS-GSM	36.97	33.58	31.70	30.38	29.37	28.56	26.35	23.75
BM3D	37.28	33.92	32.14	30.88	29.91	29.12	26.64	23.74
Proposed	**37.91**	**34.50**	**32.40**	**30.90**	**29.90**	**29.12**	**27.19**	**24.63**
Method	**Goldhill**							
SURE-LET	36.85	33.20	31.37	30.17	29.30	28.61	26.83	24.69
BLS-GSM	37.00	33.38	31.53	30.32	29.42	28.72	26.87	24.63
BM3D	37.14	33.62	31.86	30.72	29.85	29.16	27.08	24.45
Proposed	**38.04**	**34.57**	**32.60**	**31.32**	**30.55**	**30.02**	**28.54**	**26.18**
Method	**Man**							
SURE-LET	37.28	33.42	31.40	30.07	29.10	28.35	26.38	24.05
BLS-GSM	37.44	33.56	31.49	30.13	29.14	28.37	26.35	23.82
BM3D	37.82	33.98	31.93	30.59	29.62	28.86	26.59	23.97
Proposed	**38.12**	**34.14**	**32.16**	**30.84**	**30.03**	**29.46**	**27.72**	**25.43**

* for *SURE-LET* and *BLS_GSM*, apply redundant wavelet transform

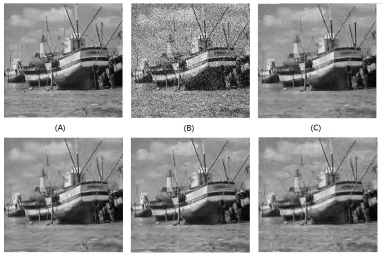

Figure 3: The *Boat* image (A) Noise-free image, (B) Noisy image with noise level of 50, (C) Result using *SURE-LET* [8] , (D) Result using *BLS_GSM* [3], (E) Result using BM3D [7], (F) Result using our method under overcomplete expansion.

6. Conclusions

We propose a simple but effective wavelet based denoising method. The wavelet coefficients we used for denoising operations are estimated from an improved context modeling based on the minimization of the mean squared error. The function of soft thresholding is a sum of weighted derivatives of Gaussian where the weights are derived by adding additional offset values to an analytical close-form solution. Meanwhile, its overcomplete expansion has also been exploited by applying the classical *cycle spinning* strategy so as to minimize the undesired Pseudo-Gibbs phenomena introduced by the standard orthogonal wavelet transform. The novelty of this approach is the two step processing scheme: improved context modeling followed by the optimization of soft-thresholding function. The concatenation of two steps of the proposed denoising approach yields preferable results in term of PSNR.

References

1. D. L. Donoho and I. M. Johnstone, "Ideal spatial adaptation via wavelet shrinkage," *Biometrika*, vol.81, pp. 425-455, 1994.
2. D. L. Donoho and I. M. Johnstone, "Adapting to unknown smoothness via wavelet shrinkage," *J. Amer. Statist. Assoc.*, vol. 90, no. 432, pp.1200-1224, Dec. 1995.
3. J. Portilla, V. Strela, M. J. Wainwright, and E. P. Simoncelli, "Image denoising using scale mixtures of gaussians in the wavelet domain," *IEEE Trans. Image Process.*, vol. 12, no. 11, pp. 1338–1351, Nov. 2003.
4. S. G. Chang, B. Yu and M. Vetterli, "Spatially adaptive wavelet thresholding with context modeling for image denoising," *IEEE Trans. Image Process.*,vol. 9, no.9, Sep. 2000.
5. F. Luisier, T. Blu and M. Unser, "A new SURE approach to image denoising: interscale orthonormal wavelet thresholding," *IEEE Trans. Image Process.*,vol. 16, no.3, Mar. 2007.
6. R. R. Coifman and D.L. Donoho, "Translation-invariant de-noising," *Wavelets and Statistics*, A. Antoniadis and G. Oppenheim eds., Spriger-Verlag Lecture Notes, 1995.
7. K. Dabov, A. Foi, V. Katkovnik, and K. Egiazarian, " Image denoising by sparse 3D transform-domain collaborative filtering," *IEEE Trans. Image Process.*, vol. 16, no. 8, Aug. 2007.
8. T. Blu and F. Luisier, "The SURE-LET approach to image denoising," *IEEE Trans. Image Process.*, vol. 16, no. 11, pp. 2778-2786, Nov. 2007.

UNIVERSITY OF Cincinnati